

Some Further Consideration for the Image Retrieving of Synthetic Aperture Radiometer

Hao Liu, Ji Wu, Qiong Wu

National Microwave Remote Sensing Laboratory,
Center for Space Science and Applied Research, Chinese Academy of Sciences,
P.O. Box 8701, Beijing, China, 100080
Phone: +86 10 6258 2778, Fax: +86 10 6252 8127, Email: liu_how@nmrs.ac.cn

Abstract: In this paper, theoretical channels model of Synthetic Aperture Radiometer is presented. Based on this model, how amplitude imbalance, phase imbalance and mutual coupling between the different channels effect brightness temperature image retrieving is analyzed. The computer simulation results are also presented to find out the cause of the along-track streaks usually appeared in the retrieved brightness temperature image. In addition, a new system calibration approach is introduced to solve this problem.

Keywords: synthetic aperture radiometer; imbalance; mutual coupling; calibration; image retrieving

1. Introduction

As a passive remote sensor, microwave radiometer will be used widely in remote sensing application. The applied fields of conventional microwave radiometer are limited because of the low spatial resolution. Synthetic aperture technology in radio astronomy is introduced into microwave radiometer to enhance the spatial resolution since 1980's [1]. The most successful and exciting progresses of this technology have been achieved in one dimensional case, such as ESTAR [2]. A 6 channels C-band synthetic aperture radiometer has been also developed by Center for Space Science and Applied Research (CSSAR), Chinese Academy of Sciences (CAS) [3], while an 8 channels X-band system is now under developing.

Fig. 1 illustrates a typical system configuration of one dimensional synthetic aperture radiometer.

In the block diagram, each of P antenna elements corresponds to an independent receiver. Some specific pairs of outputs of P receivers are correlated to get

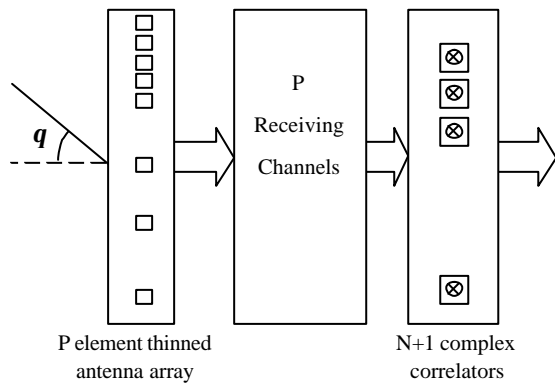


Fig.1. Block Diagram of One Dimensional Synthetic Aperture Radiometer

$N+1$ visibility functions (N cross-correlated and one self-correlated).

Using discrete Fourier transform or some other numerical algorithms, we can retrieve the brightness temperature image from these visibility functions [1][4].

The Fourier relationship between the retrieved brightness temperature and the visibility function can be written as follow:

$$V(n) = \int_{\text{视场}} T(\mathbf{q}) \exp(j \cdot 2pn \frac{\Delta d}{l} \sin \mathbf{q}) d\mathbf{q}, \quad (n=0,1 \dots N) \quad (1)$$

$$\hat{T}(\mathbf{q}) = \sum_{n=-N}^N V(n) \exp(-j \cdot 2pn \frac{\Delta d}{l} \sin \mathbf{q}), \quad (2)$$

where Δd is the least space of the antenna array elements. $T(\mathbf{q})$ is the real scene brightness temperature, while $\hat{T}(\mathbf{q})$ is the retrieved brightness temperature. $V(-n)$ is equal to the conjugate of $V(n)$.

The Fourier relationship in (1) is determined by the configuration of thinned antenna array and the specific input channels combination of the correlators. And this ideal Fourier relationship requires the balance and incoherence of the P channels. However, ideal channels properties are impossible in practical implementation, imbalance (both amplitude and phase) and mutual coupling always exist between different channels [5]. These unideal channels properties make (1) no longer available.

We rewrite (1) in matrix formulation for convenience

$$\begin{matrix} V \\ (2N+1) \times 1 \end{matrix} = \begin{matrix} G \\ (2N+1) \times M \end{matrix} \cdot \begin{matrix} T \\ M \times 1 \end{matrix} \quad (3)$$

where G matrix is the system pulse response.

In general, the number of retrieved points M is greater than the number of visibility function sample points $2N+1$. For example, in our Xband synthetic aperture radiometer system, $P=8$, $N=19$, and $M=156$. It means that (3) is an undetermined system of equations, and retrieving the brightness temperature is equivalent to finding the minimum norm solution of (3). According to the Backus-Gilbert method, the retrieved brightness temperature can be written as the linear combinations of the visibility functions

$$\hat{T} = C \cdot V = G^T (GG^T)^{-1} \cdot V \quad (4)$$

where $C = G^T (GG^T)^{-1}$ is the pseudo-inverse of G matrix.

Nevertheless, in practice many unexpected along-track streaks always appear in the retrieved image. These streaks highly deteriorate the quality of retrieved image. To find out the cause of these streaks and reduce them is a very important task in the image retrieving of synthetic aperture radiometer.

2 . Channels Model and Error Analysis

The term 'channel' used here means the microwave front-end and the IF amplifier. This part can be seen as a linear system, so a complex matrix A can be defined to characterize the channels

$$A = \begin{bmatrix} a_{11} & a_{12} & \cdots & a_{1P} \\ a_{21} & a_{22} & \cdots & a_{2P} \\ \vdots & \vdots & \ddots & \vdots \\ a_{P1} & a_{P2} & \cdots & a_{PP} \end{bmatrix} \quad (5)$$

A is the normalized transmission characteristic matrix of the channels. The elements of A matrix is $a_{ij}(\mathbf{w}) = |a_{ij}(\mathbf{w})| \cdot e^{j\mathbf{f}_{ij}(\mathbf{w})}$. If $i = j$, $|a_{ij}(\mathbf{w})|$ and $\mathbf{f}_{ij}(\mathbf{w})$ represent the gain and the phase shift of the channel i respectively, else $a_{ij}(\mathbf{w})$ represents the mutual coupling between i th and j th channel. Since the gain of channel itself is always much greater than the mutual coupling between different channels, A matrix is a diagonally dominant matrix. According to reciprocity principle, $|a_{ij}| = |a_{ji}|$, $\mathbf{f}_{ij} = \mathbf{f}_{ji}$, the matrix can be simplified. Furthermore, transmission characteristics of the channels are supposed to be independent of the frequency in the bandwidth.

1) Ideal channels

A is an identity matrix, $a_{ij} = \begin{cases} 1, & i = j \\ 0, & i \neq j \end{cases}$. The

visibility function and the brightness temperature satisfy the Fourier relationship. With referenced to (1), one finds that G matrix should be calculated as follow

$$G(n, m) = \exp(j \cdot 2\mathbf{p}n \frac{\Delta d}{I} \sin \mathbf{q}_m), \quad (n = -N; \cdots 0; \cdots N; m=1, \cdots M) \quad (6)$$

2) Unideal channels

When the channels are unideal, these unideal channels characteristics (A matrix) must be converted into the G matrix. For example, in our Xband system, $P=8$, $N=19$, and $M=156$. Set the position of first antenna unit as the origin of coordinates, the 8 antenna units are placed at $0, \Delta d, 2\Delta d, 3\Delta d, 4\Delta d, 9\Delta d, 14\Delta d, 19\Delta d$ respectively, where $\Delta d = 0.735 I$.

Let $D = [0 \ 1 \ 2 \ 3 \ 4 \ 9 \ 14 \ 19]^T$ and $E = \exp(j \cdot 2\mathbf{p} \cdot D \cdot \frac{\Delta d}{I} \sin \mathbf{q}_m)$, G matrix can be given as follow

$$G(n, m) = (A_k E)^* \cdot (A_l E), \quad (n = 0; \cdots N; m=1, \cdots M) \quad (7)$$

$$G(-n, m) = G^*(n, m)$$

where $'$ means transpose, $*$ means conjugate. Subscripts k and l represent the two input channels of the n th correlator, it means that $D(l) - D(k) = n$. Vectors A_k and A_l are the k th and l th row of A matrix.

Expand (7) to get a new G matrix expression

$$G(n, m) = K_n \cdot \exp(j \cdot 2\mathbf{p}n \frac{\Delta d}{I} \sin \mathbf{q}_m) + C_{nm} \quad (n = 0; \cdots N; m=1, \cdots M) \quad (8)$$

where $K_n = a_{kk} a_{ll}$,

$$C_{nm} = G(n, m) - a_{kk} a_{ll} \exp(j \cdot 2\mathbf{p}n \frac{\Delta d}{I} \sin \mathbf{q}_m)$$

By comparing (8) with (6), it is obviously that how unideal channels characteristics effect image retrieving: the imbalance between different channels results in a complex weighting (K_n) on each visibility function; and the mutual coupling makes each visibility function add an offset (C_{nm}) contributed by other baselines' visibility functions.

3 . Simulation Results

In this section, several computer simulation results of brightness temperature retrieving will be presented to show the effects of unideal channels characteristics apparently.

1) Effects of Imbalance

Two one dimensional simulations are conducted to demonstrate the effects of amplitude and phase imbalance respectively. In both simulations, channel 2 is used as an ideal reference channel. Tab.1 is the parameters used in simulations.

Fig.2 shows the simulation results of amplitude imbalance effects, while Fig.3 shows the phase imbalance effects. In both figures, the dash-dot line represents the original real brightness temperature distribution; the dotted line is the retrieved brightness temperature with the channels biases as shown in Tab.1(using G matrix in (6)); and the solid line is the

Tab.1 Amplitude & Phase Imbalance between Channels

Channel	1	2	3	4	5	6	7	8
Amplitude (db)	1.42	0	-0.88	-1.75	-1.94	0.25	0.81	1.01
Phase (Degree)	0.60	0	-5.45	8.70	0.35	-0.81	5.53	4.68

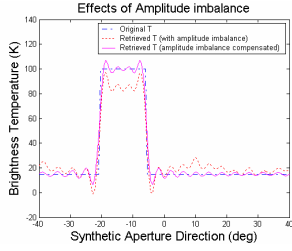


Fig.2. Effects of Amplitude Imbalance

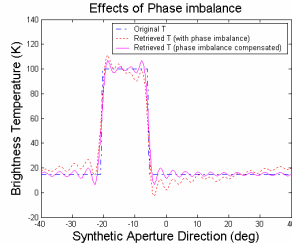


Fig.3. Effects of Phase Imbalance

retrieved brightness temperature with the channels biases be compensated (using G matrix in (8)). Compared the three brightness temperature distribution, the effect of channels imbalance can be seen apparently.

2) Effects of Mutual Coupling

Two dimensional image retrieving simulation is conducted to demonstrate the effects of mutual coupling. Fig.4 is a scene of Landsat image made of Yellow River near Xi'an, used here as a source map of real brightness temperature distribution. In the simulation, the mutual coupling between each pair of channels is generated randomly and limited below -30db. Fig.5 is the retrieved image with mutual coupling (using G matrix in (6)). In Fig.5, many streaks can be seen in the real aperture direction, which is very similar with those appeared in the experimental retrieved image. These streaks can be attributed to the offset value C_{nm} caused by mutual coupling. Fig.6 is the image retrieved by G matrix in (8), in which streaks are removed effectively.

4 . Calibration Approach

Based on the discussion above, one should realize that to achieve the accurate system response, G matrix, is the core problem of the image retrieving and system calibration. There are two conventional techniques for G Matrix measurement [4]: one is to direct measuring the point source in the antenna range in anechoic chamber, and the other is to using open water as a reference. Considering the convenience and accuracy, both of them are not perfect for practical in situ use. In this paper, a new system calibration approach is presented. Using P digital I-Q vector modulators to simulate the point source in the antenna range, we can get more accurate G matrix to retrieve the brightness temperature image and reduce the streaks to a very low level.

Using our X-band system for example: to simulate a point source in the antenna range in \mathbf{q}_m direction as shown in Fig.1, the phase shift of the n th antenna element should be calculated as

$$\Delta f(n, m) = \text{mod}\left(2\mathbf{p} \cdot D(n) \cdot \frac{\Delta d}{l} \cdot \sin \mathbf{q}_m, 2\mathbf{p}\right) \quad (n=1, \dots, 8; m=1, \dots, 156) \quad (9)$$

Adding these 156 sets of phase shifts in (9) to 8 branches of coherent noises come from one same noise source, injecting these 8 branches of noises to the input

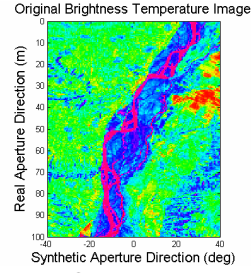


Fig.4. Original Brightness Temperature Image

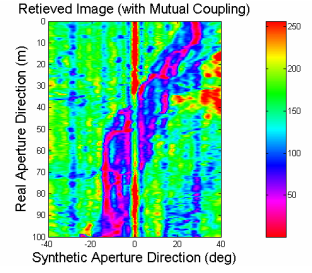


Fig.5. Retrieved Image (with Mutual Coupling)

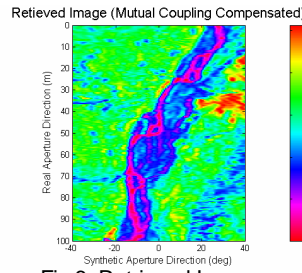


Fig.6. Retrieved Image (Mutual Coupling Compensated)

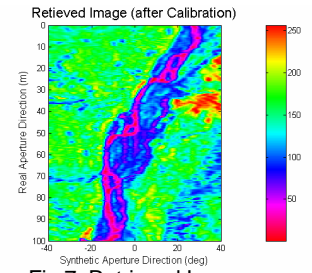


Fig.7. Retrieved Image (after Calibration)

ports of 8 front-ends of the X-band system, we can get G matrix from output visibility functions directly [4].

Fig.7 is the simulation result of image retrieved by the G matrix measured by this new calibration approach, in which the phase control accuracy of the digital I-Q vector modulators are supposed to be 3 degrees.

5 . Conclusion

The unideal channels model of synthetic aperture radiometer is analyzed in this paper. Conclusion has been made that mutual coupling between different channels contributes to the streaks appeared in retrieved image. A new calibration approach is also introduced in this paper and proved to be effective.

Reference

- [1] C. S. Ruf, C. T. Swift, A. B. Tanner and D. M. Le Vine, Interferometric synthetic aperture microwave radiometry for the remote sensing of the earth, IEEE Trans. GRS, Vol.26, No.5, pp.597-611, Sep, 1988
- [2] D. M. Le Vine, A. J. Griffis, C. T. Swift, T. J. Jackson, ESTAR: A Synthetic Aperture Microwave Radiometer for Remote Sensing Applications, Proceedings of the IEEE, v 82, n 12, Dec, 1994, p 1787-1801
- [3] Xiaolong Dong, Ji Wu, Suyun Zhu, Bo sun and Jingshan Jiang, Design and implementation of CAS C-band interferometric synthetic aperture radiometer, Proceedings of IGARSS'00, 2000, Vol. II, pp866~868
- [4] A. B. Tanner, C. T. Swift, Calibration of a synthetic aperture radiometer, IEEE Trans. GRS, Vol.31, No.1, pp.257-267, Jan, 1993
- [5] DONG Xiao-long, WU Ji, JIANG Jing-shan, Analysis and Calibration of Effects on Complex Correlations from Mutual Coupling and Imbalance between Channels, ACTA ELECTRONICA SINICA, Vol. 29, No. 7, July, 2001. (In Chinese).